Diels−Alder Topochemistry via Charge-Transfer Crystals: Novel (Thermal) Single-Crystal-to-Single-Crystal Transformations

J. H. Kim, S. M. Hubig, S. V. Lindeman, and J. K. Kochi*

Contribution from the Department of Chemistry, University of Houston, Houston, Texas 77204-5641

Received June 1, 2000. Revised Manuscript Received October 24, 2000

Abstract: The solid-state [4+2] cycloaddition of anthracene to bis(*N*-ethylimino)-1,4-dithiin occurs via a unique single-phase topochemical reaction in the intermolecular (1:1) charge-transfer crystal. The thermal heteromolecular solid-state condensation involves the entire crystal, and this rare crystalline event follows topochemical control during the entire cycloaddition. As a result, a new crystalline modification of the Diels−Alder product is formed with a crystal-packing similar to that of the starting charge-transfer crystal but very different from that of the (thermodynamically favored) product modification obtained from solution-phase crystallization. Such a single-phase transformation is readily monitored by X-ray crystallography at various conversion stages, and the temporal changes in crystallographic parameters are correlated with temperature-dependent (solid-state) kinetic data that are obtained by ^{1}H NMR spectroscopy at various reaction times. Thus, an acceleration of the solid-state reaction over time is found which results from a progressive lowering of the activation barrier for cycloaddition in a single crystal as it slowly and homogeneously converts from the reactant to the product lattice.

Introduction

Solid-state chemistry has attracted much attention as an approach to carry out chemical reactions with high regio- and/or stereoselectivity under environmentally friendly (solvent-free) conditions.[1−5] Enhanced stereoselectivity for enantiomeric (pure) synthesis[4,6] is the result of the topochemical control[7] of the solid-state reaction. In other words, the crystal lattice of the starting material controls the relative orientation of the neighboring reactant molecules and, thus, their reactivity because molecular motion is restricted in the solid state, as compared to solution-phase reactions. Recent studies have shown that the reactivity of organic crystals is also strongly affected by the free space surrounding the reactant molecules, which allows certain degrees of molecular motion in the crystal lattices. As a result, the reaction cavity and the lattice energy are primary factors that control solid-state reactivity.[8−10]

In most solid-state reactions, the formation of products distorts the crystal lattice of the starting material to such a degree that the crystal structure of the reactants collapses at rather low conversions, and a new crystal phase of the product grows heterogeneously inside the original crystal. As a result, the topochemical control based on the crystal lattice of the starting material fades away, and the reaction is mostly controlled by the free-energy changes that are due to lattice transformations. In such cases, the reaction progresses at the interface between reactant and product crystal lattices, which complicates thermodynamic and kinetic evaluations.

To circumvent the above-mentioned problems, it is highly desirable to design reactive crystalline materials in which the chemical transformations do not significantly distort the original reactant crystal lattice. As a consequence, topochemical control remains an important factor throughout the entire solid-state reaction, even at high conversions. To achieve such reaction conditions, the reactant crystal lattice should contain substantial amounts of "spare" free space that accommodates a controlled motion of the reactant molecules during the reaction. Such crystalline materials not only follow the topochemical control ideally from the beginning to the end of the reaction, but their solid-state transformation is also readily monitored by X-ray crystallography because the entire crystal converts homogeneously from a reactant to a product single crystal via a solid solution.[11]

There are only a few examples of solid-state reactions that occur as a single-phase transformation.[13] Moreover, most solid-state reactions known in the literature represent homomolecular

(1) Addadi, L.; Mil, J. V.; Lahav, M. *J. Am. Chem. Soc.* **1982**, *104*, 3422. See also: Mil, J. V.; Addadi, L.; Gati E.; Lahav, M. *J. Am. Chem. Soc.* **1982**, *104*, 3429.

(2) Cohen, M. D. *Tetrahedron* **1987**, *43*, 1211.

(3) Zimmerman, H. E.; Zuraw, M. J. *J. Am. Chem. Soc.* **1989**, *111*, 7974.

(4) (a) Chung, C. M.; Hasegawa, M. *J. Am. Chem. Soc.* **1991**, *113*, 7311. (b) Tanaka, K.; Toda, F.; Mochizaki, E.; Yasui, N.; Kai, Y.; Miyahara, I.; Hirotsu, K. *Angew. Chem., Int. Ed. Engl.* **1999**, *38*, 3523.

(5) McCullough, J. D., Jr.; Curtin, D. Y.; Paul, I. C. *J. Am. Chem. Soc.* **1972**, *94*, 874.

(6) Addadi, L.; Lahav, M. *J. Am. Chem. Soc.* **1979**, *101*, 2152.

(7) (a) Schmidt, G. M. *J. Pure Appl. Chem.* **1971**, *27*, 647. (b) Cohen, M. D.; Schmidt, G. M. J.; Sonntag, F. I. *J. Chem. Soc.* **1964**, 2000. (c) Fu, T. Y.; Liu, Z.; Scheffer, J. R.; Trotter, J. *J. Am. Chem. Soc.* **1993**, *115*, 12202. (d) Enkelmann, V.; Wegner, G.; Novak, K.; Wagener, K. B. *J. Am. Chem. Soc.* **1993**, *115*, 10390.

(8) Leibovitch, M.; Olovsson, G.; Scheffer, J. R.; Trotter, J. *J. Am. Chem. Soc.* **1998**, *120*, 12755.

(9) Appel, W. K.; Jiang, Z. Q.; Scheffer, J. R.; Walsh, L. *J. Am. Chem. Soc.* **1983**, *105*, 5354.

(10) Murthy, G. S.; Arjunan, P.; Venkatesan, K.; Ramamurthy, V. *Tetrahedron* **1987**, *43*, 1225.

(11) This unusual crystalline (thermal) transformation is to be distinguished from other single-crystal-to-single-crystal transformations in which a new (product) crystalline phase grows topotactically within the original (reactant) crystal lattice. However, there have been attempts to convert heterogeneous solid-state photoreactions to a more homogeneous course by selective irradiation of the absorption tail. [See Enkelmann et al. in ref 7d and also (a) Hosomi, H.; Ohba, S.; Tanaka, K.; Toda, F. *J. Am. Chem. Soc.* **2000**, *122*, 1818, and (b) Novak, K.; Enkelmann, V.; Wegner, G.; Wagener, K. B. *Angew. Chem., Int. Ed. Engl.* **1993**, *32*, 1614.] This solid-state transformation is hereinafter referred to as a single-phase topochemical reaction.[12]

10.1021/ja001939n CCC: $20.00
Published on Web 12/09/2000

Chart 1

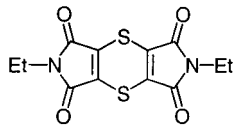

transformations such as isomerization, dimerization and polymerization.[14,15] Heteromolecular reactions such as the Diels−Alder cycloaddition in the solid state represent an experimental challenge,[16] mostly due to the fact that reactants of different sizes and/or shapes are difficult to cocrystallize into one crystal lattice. To achieve heteromolecular solid-state reactions, the following requirements are important: (i) The cocrystallized reactant molecules should have compatible shapes and sizes. (ii) The heteromolecular interactions should be stronger than the corresponding homomolecular interactions; that is, $E_{A+B} > E_{A+A}$ and E_{B+B}. We believe the latter requirement can be fulfilled by intermolecular charge-transfer interactions of appropriate electron donors and acceptors, which we have studied extensively.[17] Hydrogen bonding[18] and Coulombic attraction[19] will also aid considerably in the efficient preassembly of electron donors and acceptors in the solid state.

In this report, we describe the successful design of a solid-state reaction that results in a single-phase topochemical transformation by exploiting (i) the free space in the crystal lattice as well as (ii) the conformational flexibility of one of the reactants. This design is based on the premise that the reactant molecule must be sufficiently flexible to undergo the desired reaction without generating major steric repulsion in the crystal lattice, so that the product lattice can coexist next to the neighboring reactant lattice without discontinuity. As a good candidate for such a flexible molecule, we chose a 1,4-dithiin ring system which exhibits a high flexibility of the dihedral angle between the two S−C═C−S planes, depending on the substituents.[20] For example, the bis(imino)-substituted 1,4-dithiin in Chart 1 exhibits a planar structure, whereas the tetracyano analogue has a folded structure.[21] Moreover, 1,4-dithiins react readily with anthracene in solution to form a Diels−Alder cycloaddition product.[22] Indeed, we found that the planar structure of the 1,4-dithiin in Chart 1 facilitates the formation of charge-transfer crystals with anthracene in alternate donor−acceptor stacks. Moreover, the crystal packing is ideal for a solid-state [4 + 2] cycloaddition that finally leads to a new crystalline modification of the cycloaddition product.

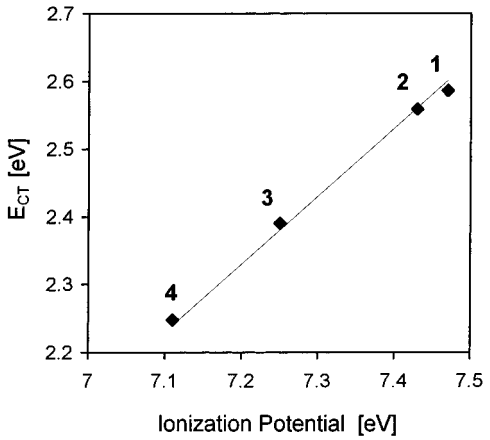

Figure 1. Mulliken correlation with a unit slope of the charge-transfer energies of EDA complexes of 1,4-dithiin with various anthracenes (**1**: 9-bromoanthracene, **2**: anthracene, **3**: 9-methylanthracene, **4**: 9,10-dimethylanthracene).

Results

1. Formation of Charge-Transfer Crystals. When solutions of bis(*N*-ethylimino)-1,4-dithiin (0.01 M) and anthracene (0.01 M) in dichloromethane were mixed, a brown color developed immediately. UV−vis spectroscopic analysis of the mixture revealed a new absorption band between 350 and 600 nm (λ_{max} = 485 nm) where neither anthracene nor the dithiin absorb. This absorption band underwent a hypsochromic shift when anthracene was replaced by its electron-poor 9-bromo analogue (λ_{max} = 481 nm), and successive bathochromic shifts when anthracene was replaced by its electron-rich 9-methyl and 9,10-dimethyl analogues (λ_{max} = 519 and 552 nm, respectively). The new absorptions were, thus, assigned to charge-transfer (CT) transitions in the intermolecular electron donor−acceptor (EDA) complexes of the various anthracenes with the 1,4-dithiin,[20b] and the linear plot in Figure 1 of the transition energies ($E = h\nu_{max} = hc/\lambda_{CT}$) versus the ionization potentials of the anthracene donors was obtained with a unit slope that was in accord with Mulliken theory.[23] The molar ratio of donor and acceptor in the CT complex was evaluated by a Job plot[24] (see Figure 2). Thus, the absorbance at λ_{CT} = 485 nm was measured for various molar fractions of anthracene and 1,4-dithiin, and the highest value was obtained for an equimolar mixture of donor and acceptor, to confirm the 1:1 complex formation.

(12) Crystalline transformations that do not lead to a new or different phase are ambiguously referred to as either homogeneous or one-phase reactions. We prefer the descriptor "monophasic" but will employ "single-phase" hereinafter as a compromise.

(13) (a) Wang, W. N.; Jones, W. *Tetrahedron* **1987**, *43*, 1273. (b) Nakanishi, H.; Jones, W.; Thomas, J. M.; Hursthouse, M. B.; Motevalli, M. *J. Phys. Chem.* **1981**, *85*, 3636. (c) Honda, K.; Nakanishi, F.; Feeder, N. *J. Am. Chem. Soc.* **1999**, *121*, 8246. (d) Ohashi, Y.; Yanagi, K.; Kurihara, T.; Sasada, Y.; Ohgo, Y. *J. Am. Chem. Soc.* **1981**, *103*, 5805 and *J. Am. Chem. Soc.* **1982**, *104*, 6353.

(14) Homomolecular reactions involve a single reactant, irrespective of the molecularity, whereas heteromolecular reactions require two or more different reactants.

(15) For recent reviews, see: (a) Tanaka, K.; Toda, F. *Chem. Rev.* **2000**, *100*, 1025. (b) Enkelmann, V. *Adv. Polym. Sci.* **1984**, *63*, 91. (c) Keating, A. E.; Garcia-Garibay, M. A. In *Organic and Inorganic Photochemistry*; Ramamurthy, V., Schanze, K. S., Eds.; Marcel Dekker: New York, 1998; pp 195−248. See also: (d) Desiraju, G. R.; Paul, I. C.; Curtin, D. Y. *J. Am. Chem. Soc.* **1977**, *99*, 1594. (e) Parkinson, G. M.; Thomas, J. M.; Williams, J. O.; Goringe, M. J.; Hobbs, L. W. *J. Chem. Soc., Perkin II*, **1976**, 836. (f) Stezowski, J. J.; Peachey, N. M.; Goebel, P.; Eckhardt, C. J. *J. Am. Chem. Soc.* **1993**, *115*, 6499. (g) Wegner, G. *Makromol. Chem.* **1971**, *145*, 85. (h) Xiao, J.; Yang, M.; Lauher, J. W.; Fowler, F. W. *Angew. Chem., Int. Ed. Engl.* **2000**, *39*, 2132. (i) Foley, J. L.; Li, L.; Sandman, D. J.; Vela, M. J.; Foxman, B. M.; Albro, R.; Eckhardt, C. J. *J. Am. Chem. Soc.*, **1999**, *121*, 7262.

(16) Most of the single-phase transformations observed heretofore are not thermal, but rather are photoreactions which involve a single reactant, such as the photoisomerization recently reported by Carducci, M. D.; Pressprich, M. R.; Coppens, P. *J. Am. Chem. Soc.* **1997**, *119*, 2669.

(17) (a) Rathore, R.; Lindeman, S. V.; Kochi, J. K. *J. Am. Chem. Soc.* **1997**, *119*, 9393. (b) Bosch, E.; Hubig, S. M.; Lindeman, S. V.; Kochi, J. K. *J. Org. Chem.* **1998**, *63*, 592 and references therein.

(18) (a) Desiraju, G. R. *Angew. Chem., Int. Ed. Engl.* **1995**, *34*, 2311. (b) Feldman, K. S.; Campbell, R. F.; Saunders, J. C.; Ahn, C.; Masters, K. M. *J. Org. Chem.* **1997**, *62*, 8814.

(19) Coates, G. W.; Dunn, A. R.; Henling, L. M.; Ziller, J. W.; Lobkovsky, E. B.; Grubbs, R. H. *J. Am. Chem. Soc.* **1998**, *120*, 3641.

(20) (a) Howell, P. A.; Curtis, R. M.; Lipscomb, W. N. *Acta Crystallogr.* **1954**, *7*, 498. (b) Hayakawa, K.; Mibu, N.; Osawa, E.; Kanematsu, K. *J. Am. Chem. Soc.* **1982**, *104*, 7136.

(21) Dollase, W. A. *J. Am. Chem. Soc.* **1965**, *87*, 979.

(22) Draber, W. *Chem. Ber.* **1967**, *100*, 1559.

(23) (a) The charge-transfer absorption (λ_{CT}) generally occurs in the UV−vis region, with hc/λ_{CT} = IP − EA − ω, where IP is the ionization potential of the donor, and EA is the electron affinity of the electron acceptor. (b) Mulliken, R. S. *J. Am. Chem. Soc.* **1952**, *74*, 811.

(24) Job, P. *Ann. Chem.* **1928**, *9*, 113.

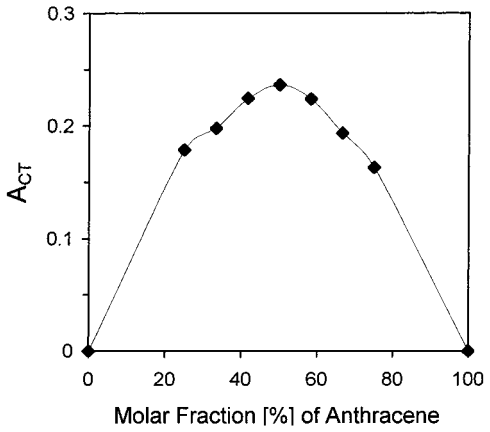

Figure 2. Job plot for various anthracene−1,4-dithiin mixtures.

The 1:1 complex of anthracene and 1,4-dithiin was isolated in crystalline form as brown needles by evaporation of the solvent. Most importantly, the diffuse reflectance spectrum of the brown crystals (taken as a 5% mull in a potassium hexafluorophosphate matrix) appears to be the same as the absorption spectrum of the charge-transfer complex taken above in dichloromethane solution (Figure 3).

Slow evaporation of dichloromethane from an equimolar mixture of anthracene and the dithiin at low temperature (−4 °C) resulted in the formation of single crystals that were suitable for X-ray crystallographic analysis. X-ray crystallography revealed the packing of the cofacially oriented 1,4-dithiin and anthracene in infinite alternate stacks along the crystallographic *x*-axis (see Figure 4A). Such a stacking was facilitated by the planar structure of the dithiin with the two ethyl groups in trans configuration (see Figure 4A). The donor−acceptor stacks were linked to each other along the crystallographic *y*-axis through hydrogen-bonding contacts between the carbonyl group of the 1,4-dithiin and the hydrogen in the 9-position of the anthracene (see Figure 4B). Such C−H···O interactions have only recently been accepted as a new type of hydrogen bond with significant structural effects.[25] Thus, the observed H···O distance of $d =$ 2.46 Å, which is significantly shorter than the sum of the van der Waals radii of hydrogen and oxygen ($d_{vdW} = 2.72$ Å), clearly reveals such interactions (the corresponding C···O distance is 3.33 Å, and the CH···O angle is 144°). Moreover, the ethylene groups of the 1,4-dithiin approach the centers of the anthracenes above and below the 1,4-dithiin with a separation of $d = 3.34$ Å (Note the actual distances between carbons in the pair of incipient C−C bonds are 3.39 and 3.50 Å.) This close cofacial orientation of 1,4-dithiin and anthracene represents an ideal arrangement for solid-state Diels−Alder cycloadditions in the charge-transfer crystal.

2. Solid-State Diels−Alder Reaction. In benzene solution, bis(*N*-ethylimino)-1,4-dithiin (**1**) reacts with anthracene (**2**) to form the Diels−Alder product **3** (see Scheme 1).[20b] This reaction has been shown to occur via the formation of the 1:1 charge-transfer (CT) complex of **1** and **2**. Similarly, the CT crystals of the acceptor **1** and the donor **2** that were described in the previous section undergo a slow reaction at room temperature (in the dark) within 2 months to give the same product (**3**). Concomitantly, the brown color of the crystal changed to yellow uniformly throughout the entire crystal. This thermal solid-state reaction was also carried out at higher temperatures of 50, 60, 70, and 80 °C to consistently afford the adduct **3** in quantitative yields. Our attempts to induce the solid-state reaction photochemically were uniformly unsuccessful, as also observed by Foley et al. in ref 15i.

Most importantly, the entire single crystal remained intact up to a conversion of 50%. Thereafter, the quality of the crystal slowly diminished, being converted to microcrystals of the same phase. Thus, a unique heteromolecular topochemical reaction took place which involved the entire crystal, as opposed to a new (product) single-crystal growing inside the original (reactant) single crystal, and it is, thus, referred to as a single-phase transformation. X-ray crystallographic examinations of single crystals at various degrees of conversion (0−50%), as well as powder X-ray diffraction (0−100%), confirmed this unique single-phase transformation. Thus, Figure 11 shows the X-ray powder diffraction patterns to be singularly unchanged throughout most of the thermal conversion of the donor−acceptor pair to the Diels−Alder cycloadduct in Scheme 1.[26] Such as crystallographic observation implies that all chemical transformations occur within the same crystal lattice.

X-ray-single-crystal analyses were carried out at various degrees of conversion to monitor the changes in the lattice parameters (see Table 1) and to identify the atomic movements in the reactant lattice to form the Diels−Alder cycloadduct (see Table 2).

The solid-state cycloaddition caused moderate distortions in the cell parameters on going from the reactant to the product lattice which are listed in detail in Table 1. Typically, Figure 5 illustrates these changes that occurred when the reaction was carried out isothermally at 50 °C. The cell parameters *a* and *b* at first increased slightly and then changed faster and faster after 4 h. The *c* parameter did not change much up to a conversion of 20%, but it decreased quickly at later reaction times. The same trends were found in the angles of the elementary cell, with the α and β angles increasing, but γ decreasing, over time. All of the angle changes became faster after 4 h until the single-crystal lost its quality at 6 h (see Figure 5B).

Figure 6 demonstrates the molecular changes on going from the reactant (black bonds) to the cycloadduct (white bonds). Both structures were extracted from the same X-ray data as a superposition of the crystallographically ordered starting material and the product, which was reproducibly oriented within the reactant crystal lattice without affecting the crystallographic positions of the reactant molecules.

A detailed list of the changes of atomic positions during the reaction is given in Table 2. For example, carbon atoms C_7 and C_{7A} of anthracene and C_{10} and C_{11} of the 1,4-dithiin moved by about 1.2−0.7 Å, respectively, to form the cycloadduct. Interestingly, one-half of the 1,4-dithiin moiety did not move much during the reaction, but the dihedral angle between the −S−C═C−S− and the −S−C−C−S− groups changed dramatically from 180 to 138°. Moreover, significant structural changes were found in the ethyl groups. Thus, the ethyl moiety on the bond-forming side of the 1,4-dithiin changed its orientation, which led to an overall cis conformation of the ethyl groups in the product structure.

(25) (a) Desiraju, G. R. *Acc. Chem. Res.* **1991**, *24*, 290. (b) Taylor, R.; Kennard, O. *J. Am. Chem. Soc.* **1982**, *104*, 5063.

(26) A close inspection of Figure 11 reveals the onset of a new phase after ∼70% conversion, but independent control experiments establish the new phase to result from the subsequent (much slower) "isomerization" of the metastable product phase (Figure 7A) into the thermodynamically favored crystalline form (Figure 7B). (Note also the absence of an intermediate amorphous phase, as queried by a reviewer.) In other words, in this donor−acceptor system, the chemical reaction occurs homogeneously (in a single phase) under continuous topochemical control. It is important to emphasize that the phase separation observed at >70% conversion is an independent process which only follows, and is separate from, the topochemical process; it becomes noticeable only at relatively longer times (high chemical conversions).

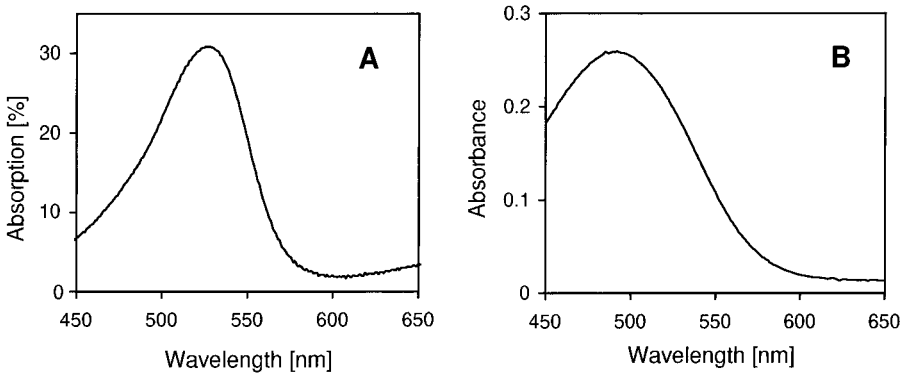

Figure 3. Solid-state reflectance spectrum (A) and absorption spectrum in dichloromethane solution (B) of the 1:1 EDA complex of anthracene and 1,4-dithiin.

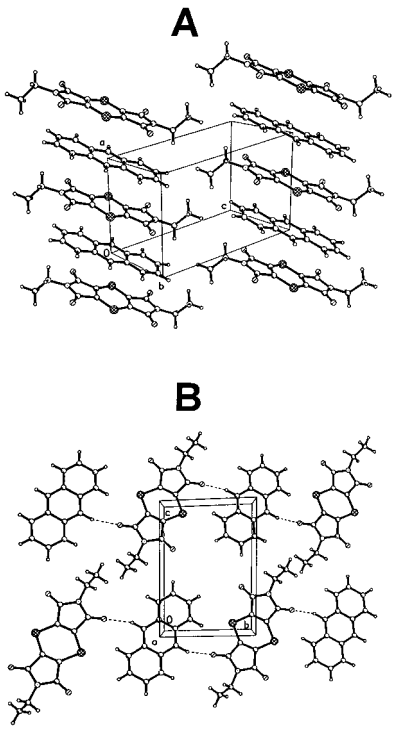

Figure 4. Crystal structure of the charge-transfer complex of 1,4-dithiin and anthracene showing (A) alternate donor−acceptor stacks and (B) hydrogen bonding between anthracene and 1,4-dithiin (see text).

Scheme 1

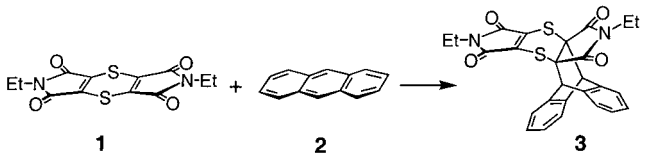

The crystal structure of the cycloaddition product obtained from the solid-state reaction was compared to that obtained from the solution-phase reaction (see Figure 7). Thus, the topochemically formed product showed a crystal packing that was very similar to the original anthracene−1,4-dithiin cocrystal with the infinite alternate arrangement of anthracene and 1,4-dithiin moieties. In contrast, the crystal structure of the cycloaddition product from a solution-phase reaction showed a dimeric packing with two cycloaddition products oriented in opposite directions, which led to a 1,4-dithiin−anthracene−anthracene−1,4-dithiin sequence. This modification exhibited a density of $\rho = 1.454$, which was similar to that of the anthracene−1,4-dithiin CT crystal ($\rho = 1.457$) but significantly higher than that of the solid-state modification ($\rho = 1.428$ at 50% conversion).

3. Kinetics of the Solid-State Reaction. The solid-state reaction of the anthracene−1,4-dithiin CT crystals was carried out at four temperatures (viz. 50, 60, 70, and 80 °C), and the conversion was monitored by ^{1}H NMR spectroscopy (see the Experimental Section). Plots of the conversion versus time for various temperatures are shown in Figure 8. First, we note that the rate of conversion *increased* with temperature. In other words, the half-life of the starting materials became shorter at higher temperature, namely, 140 min at 60 °C, 47 min at 70 °C, and 20 min at 80 °C. Interestingly, the conversion increased linearly with time at 70 °C and 80 °C. However at 60 °C, the conversion changed linearly with time only at the beginning of the reaction (until 20% conversion). At a later stage of the reaction, the rate of conversion increased and ultimately led to a rate of conversion twice as high as that at the initial stage of the reaction.

The solid-state reactions were evaluated as first-order reactions. Thus, plots of $\ln(C/C_0)$ versus time were utilized to obtain rate constants at various temperatures (see Figure 9). At the beginning of the reaction (up to 20% conversion), the plot was linear, but at conversions higher than 20%, the rates became faster and faster. First-order rate constants (k_1) were evaluated at various conversions, and as shown in Table 3, the rate constants k_1 increased with conversion.

To compare the solid-state kinetic behavior to that in solution, the preequilibrium constant (K) and the first-order rate constant (k_1, see Scheme 2) were determined in chloroform solution. Rate measurements in solution were conducted by the method of Osawa et al.,[20b] and the results are also presented in Table 3.

At the beginning of the reaction, the solid-state reaction was 16 times slower than that in the solution phase at the same temperature. However, the reaction rate increased with conversion, ultimately leading to similar values for solid-state and solution-phase reactions. Moreover, the effective activation energies (E_A) for the solid-state reaction were determined with the aid of Arrhenius plots of the rate constants versus the reciprocal temperature, and the results are given in Table 3. At the beginning of the reaction, E_A of the solid-state reaction was more than twice as large as that of the solution reaction. However, E_A decreased gradually during the solid-state reaction, finally reaching a value similar to that of the solution-phase reaction. This change of E_A during the solid-state reaction is shown in Figure 10.

Discussion

The solid-state [4 + 2] cycloaddition between anthracene and bis(*N*-ethylimino)-1,4-dithiin represents a rare example of a

Table 1. Principal Crystallographic Parameters of (a) the CT Crystal of Anthracene and 1,4-Dithiin at −150 °C, Including Changes During the Thermal Solid-State Reaction at 50 °C, and (b) the Cycloadduct Obtained from the Solution-Phase Reaction

Brutto formula		($C_{14}H_{10} + C_{12}H_{10}N_2O_4S_2 \rightarrow C_{26}H_{20}N_2O_4S_2$)[a]			($C_{26}H_{20}N_2O_4S_2$)[b]
MW		488.56			488.56
crystal symmetry		triclinic			monoclinic
		$P\bar{1}$; $Z = 1$			$P2_1/c$, $Z = 4$
degree of conversion[c]	0	9.9(3)	18.5(3)	51.5(8)	
color	red	red	orange	orange-yellow	yellow
a, Å	7.2647(2)	7.2963(5)	7.3366(5)	7.448(2)	12.951(1)
b, Å	7.3961(2)	7.3998(5)	7.4234(6)	7.472(2)	21.670(2)
c, Å	10.4962(2)	10.4905(8)	10.4827(8)	10.376(2)	8.2461(9)
α, deg	87.950(1)	88.134(2)	88.256(2)	88.831(5)	90
β, deg	84.065(1)	84.647(2)	85.090(2)	86.997(6)	105.299(2)
γ, deg	83.086(1)	82.805(2)	82.415(2)	79.862(7)	90
V, Å^3	556.71(2)	559.36(7)	563.74(7)	568.2(2)	2232.3(4)
D_c, g cm^{-3}	1.457	1.450	1.439	1.428	1.454
total reflections	7151	7952	8007	4468	26316
nonequivalent reflections	4877	4727	4758	2316	9898
obs. reflections [I > 2σ (I)]	3826	3174	3016	1193	6296
R_1	0.0602	0.0433	0.0453	0.0631	0.0501
wR_2	0.1429	0.0998	0.1040	0.1605	0.1179

[a] CT crystals at different degrees of conversion at typically 50 °C. [b] Product obtained from solution. [c] Conversion [%] in the solid-state reaction, as determined by X-ray diffraction.

Table 2. Typical Changes in the Atomic Positions During the Cycloaddition Reaction

anthracene		1,4-dithiin			
reactant[a] → product[b]	*d*[c]	reactant[d] → product[e]	*d*[c]	reactant[d] → product[e]	*d*[c]
$C_1 \rightarrow C_{1X}$	0.36	$S_1 \rightarrow S_{1X}$	0.31	$C_{8A}{}^f \rightarrow C_{8Y}$	0.29
$C_2 \rightarrow C_{2X}$	0.36	$O_1 \rightarrow O_{1X}$	0.30	$C_{9A}{}^f \rightarrow C_{9Y}$	0.23
$C_3 \rightarrow C_{3X}$	0.34	$O_2 \rightarrow O_{2X}$	0.37	$C_{10A}{}^f \rightarrow C_{10Y}$	0.31
$C_4 \rightarrow C_{4X}$	0.34	$N_1 \rightarrow N_{1X}$	0.45	$C_{11A}{}^f \rightarrow C_{11Y}$	0.30
$C_5 \rightarrow C_{5X}$	0.74	$C_8 \rightarrow C_{8X}$	0.25	$C_{12A} \rightarrow C_{12Y}$	0.18
$C_6 \rightarrow C_{6X}$	0.73	$C_9 \rightarrow C_{9X}$	0.29	$C_{13A}{}^f \rightarrow C_{13Y}$	0.28
$C_7 \rightarrow C_{7X}$	1.23	$C_{10} \rightarrow C_{10X}$	0.70		
$C_{1A}{}^f \rightarrow C_{1Y}$	0.35	$C_{11} \rightarrow C_{11X}$	0.64		
$C_{2A}{}^f \rightarrow C_{2Y}$	0.47	$C_{12} \rightarrow C_{12X}$	1.10		
$C_{3A}{}^f \rightarrow C_{3Y}$	0.41	$C_{13} \rightarrow C_{13X}$	1.28		
$C_{4A}{}^f \rightarrow C_{4Y}$	0.22	$S_{1A}{}^f \rightarrow S_{1Y}$	0.47		
$C_{5A}{}^f \rightarrow C_{5Y}$	0.68	$O_{1A}{}^f \rightarrow O_{1Y}$	0.28		
$C_{6A}{}^f \rightarrow C_{6Y}$	0.67	$O_{2A}{}^f \rightarrow O_{2Y}$	0.26		
$C_{7A}{}^f \rightarrow C_{7Y}$	1.24	$N_{1A}{}^f \rightarrow N_{1Y}$	0.27		

[a] Atoms of reactant anthracene molecule. [b] Atoms of product anthracene moiety. [c] Distance, Å, between atomic positions before and after reaction. [d] Atoms of reactant 1,4-dithiin molecule. [e] Atoms of product 1,4-dithiin moiety. [f] Atoms C_{1A} through C_{7A} and S_{1A} through C_{13A} are symmetrical equivalents of atoms C_1 through C_7 and S_1 through C_{13}, respectively, by inversion centers.

thermal single-phase transformation which occurs over the entire single crystal without breakdown of the crystal lattice or the formation of a new crystal phase within the original crystal. Such a single-phase transformation is based on the successive replacement of reactant molecules by the cycloadduct, with only minor changes in the cell parameters. As a result, X-ray crystallographic examination leads to an exact superposition of reactant and product molecules, as illustrated in Figure 6. Most importantly, this single-phase topochemical transformation leads to a new (metastable) crystalline modification of the cycloaddition product, as revealed by the comparison to the crystal structure of the same Diels−Alder product obtained from the solution-phase reaction (see Figure 7).[26] Thus, the new modification exhibits a packing very similar to the original cocrystal with anthracene and 1,4-dithiin moieties in infinite, alternate stacks. In contrast, the crystal structure of the product modification that was obtained from solution shows a completely different lattice with dimeric arrangement of the cycloaddition product. This packing is thermodynamically more favored because it exhibits a higher density and, thus, a closer packing. Moreover, we need to emphasize that the two crystalline modifications of the cycloaddition product that were obtained from the solid-state or the solution-phase reaction are formed from molecules of identical structure, that is, in both cases, the ethyl groups are in the cis conformation, and the folding angles in the 1,4-dithiin moiety are the same.

This unique solid-state reaction is based on various critical factors, which are discussed in detail as follows: Bis(*N*-ethylimino)-1,4-dithiin and anthracene form 1:1 EDA complexes in solution which can be readily isolated in crystalline form by slow evaporation of the solvent. The resulting charge-transfer single crystals exhibit a packing in alternate donor−acceptor stacks, with anthracene and 1,4-dithiin cofacially oriented, so that the ethylene bond of the 1,4-dithiin is located in the center over the anthracene moiety at a distance of $d = 3.34$ Å. During the cycloaddition, the flexible 1,4-dithiin moiety changes its dihedral angle from 180° to 138° which minimizes the atomic movements during this reaction and adjusts the volume of the product molecule to one similar to that of the two reactant molecules together. To further facilitate the cycloaddition without accommodating major changes in the cell parameters, the ethyl groups of the 1,4-dithiin moiety change their original

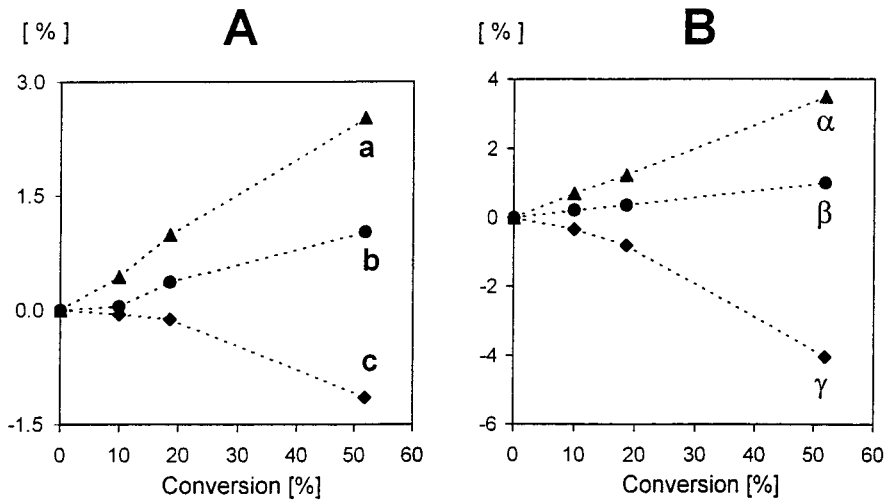

Figure 5. Relative changes in cell parameters during the thermal cycloaddition reaction (A, changes in the cell dimensions *a*, *b*, and *c*; B, changes in the angles α, *β*, and *γ*).

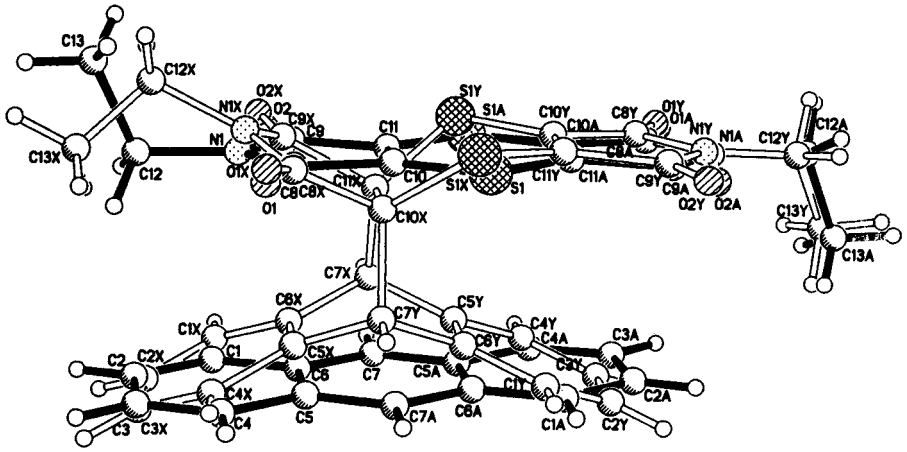

Figure 6. Changes of the atomic positions during the solid-state cycloaddition reaction (black bonds, reactants; white bonds, cycloadduct).

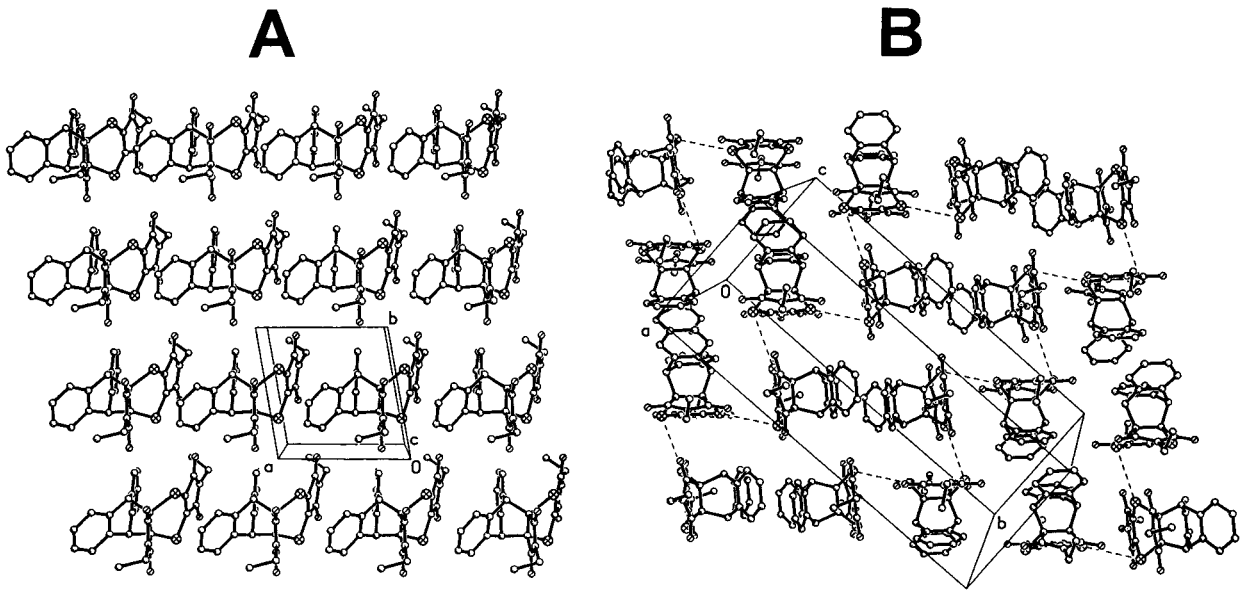

Figure 7. Crystal packing of the two modifications of the cycloaddition product obtained from (A) the solid-state and (B) the solution-phase reaction.

trans conformation to a cis conformation (see Figure 6). This structural change minimizes steric repulsions of the cycloadduct molecule within the reactant crystal lattice.[27] Thus, the product lattice slowly and homogeneously forms all over the reactant lattice without major changes in cell parameters and crystal-lattice energies.

One important feature of such single-phase transformations is the fact that they can be monitored at various stages by X-ray

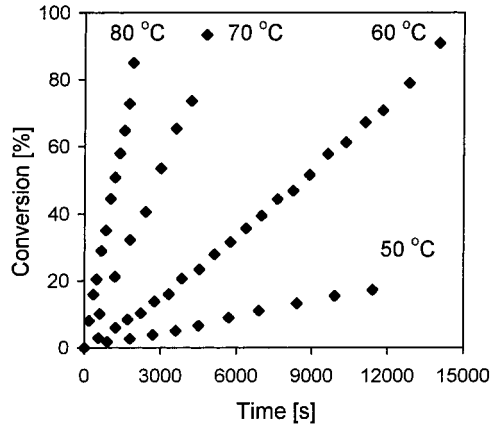

Figure 8. Conversion−time profiles for the solid-state reaction of anthracene and 1,4-dithiin monitored at various temperatures.

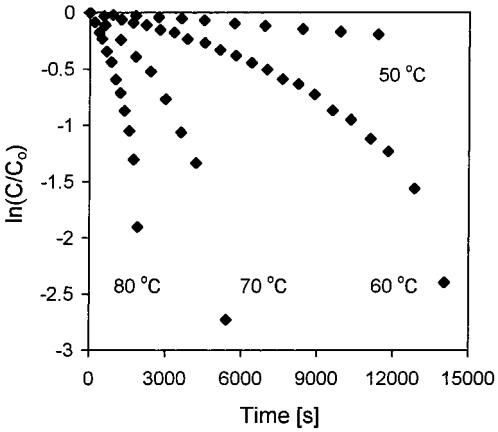

Figure 9. Kinetic evaluation of the solid-state cycloaddition as first-order reactions at various temperatures.

Table 3. Temperature-Dependent Kinetic Data of the Cycloaddition Reaction in the Solid State and in Solution

	k_1 (solid state) × 10^4 [a]					
	10%[c]	30%[c]	50%[c]	70%[c]	85%[c]	k_1 (soln) × 10^4 [b]
80 °C	4.898	6.583	7.737	12.110	25.271	
70 °C	1.987	2.358	4.079	4.730	11.160	
60 °C	0.553	0.845	1.089	2.388	6.978	
50 °C	0.189					3.08
E_A[d]	24.9	23.9	23.0	18.9	15.0	12.2 [e]

[a] First-order rate constant for solid-state reaction (s^{-1}). [b] First-order rate constant for solution-phase reaction (s^{-1}). [c] Conversion in the solid-state reaction as determined by ^{1}H NMR spectroscopy (see text). [d] Activation energy (kcal/mol). [e] Activation energy for the solution-phase reaction of the methyl-substituted bis(imino)-1,4-dithiin.[20b]

Scheme 2

$$\mathbf{1} + \mathbf{2} \underset{}{\overset{K}{\rightleftharpoons}} [\mathbf{1},\mathbf{2}]_{CT} \xrightarrow{k_1} \mathbf{3}$$

$$\frac{1}{k_{obs}} = \frac{1}{k_1} + \frac{1}{k_1 K}\left(\frac{1}{[\mathbf{2}]}\right)$$

crystallography. In our case, the single-crystal remains intact up to a conversion of 50%, which allows us to follow the change in cell parameters over time. Thus, at the beginning of the reaction, all of the cell parameters *a*, *b*, and *c* do not change significantly up to a conversion of about 20%. Beyond 20% conversion, small but significant changes are observed as

(27) In the absence of such a conformational change, the terminal methyl group would make C···C contacts with the neighboring moiety shorter than 2.4 Å.

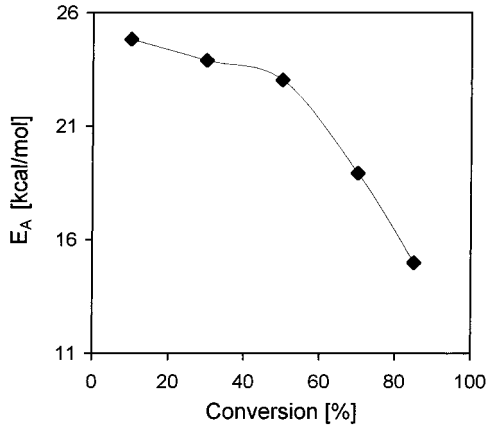

Figure 10. Change of the (effective) activation energy (E_A) during the solid-state reaction.

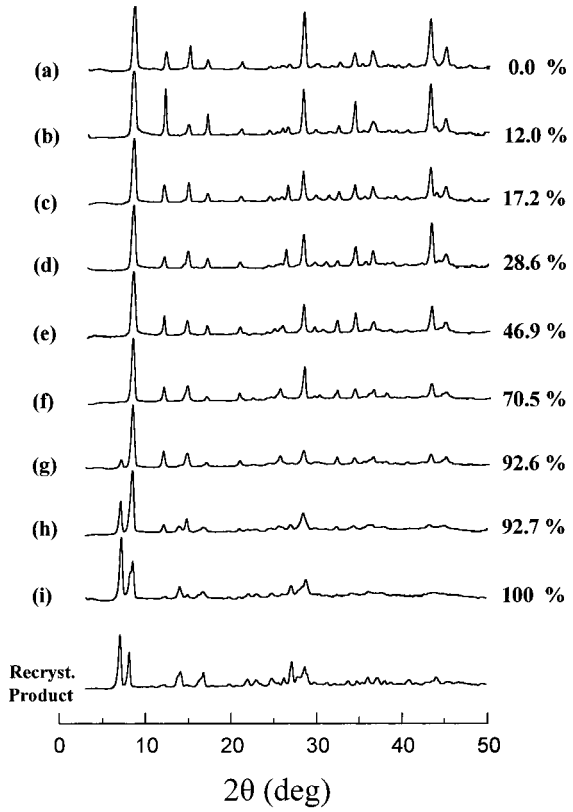

Figure 11. Temporal evolution of the powder diffraction diagram of the dithiin−anthracene complex at 50 °C, according to the protocol described in Table 4.

follows: The *a* parameter, which represents the axis of the donor−acceptor stacks, expands by 0.183 Å (2.5%) at 50% conversion due to the volume change from two planar cofacially oriented aromatic compounds to a folded cycloadduct. The *b* parameter expands by 0.076 Å (1%) due to the break-up of the hydrogen bonding observed in the reactant lattice (vide supra). The *c* parameter contracts by 0.12 Å (1.1%) during the reaction because the projected length of the folded dithiin moiety in the cycloadduct is smaller than that of the planar 1,4-dithiin starting material.

Let us now correlate these crystallographic changes over time with the kinetic behavior of the solid-state reaction, in which we note an increasing first-order rate constant with increasing conversion. The temperature study revealed that the increased rate constants are the result of decreased effective activation barriers. Thus, at the beginning of the reaction, the activation

energy is much higher than that in solution. Beyond 50% conversion, the solid-state activation energy quickly approaches the value found in solution, and after 85% conversion, the solid state and solution-phase activation energies are comparable. These changes in kinetic and thermodynamic parameters during the reaction are doubtlessly caused by changes in the crystal lattice. In the beginning, the reactant lattice is undistorted, as revealed by the unchanged cell parameters, and thus, the cycloaddition requires a rather high activation energy to accomplish the necessary atomic movements within a more-or-less unchanged reactant lattice. As a result, the rate constant in the solid state is much slower than that in solution and exhibits a strong temperature dependence. With increasing conversion, the reactant crystal lattice is slowly distorted into a product lattice, as revealed by the shifts in the cell parameters. The higher the product-lattice component in the crystal, the lower the activation energy for the atomic movements to form the cycloadduct. In other words, the product becomes thermodynamically more favorable because it fits better into the partially converted lattice. As a result, the rate constants for the cycloaddition increase with increasing conversion and ultimately lead to a value that is similar to that obtained in chloroform solution. Moreover, the final rate constant is much less temperature-dependent.

We also note that the unique solid-state cycloaddition reaction proceeds in essentially quantitative yields. This result is unexpected when one considers the fact that in alternate stacks of anthracene and 1,4-dithiin, random reactions between neighboring reactants would result in a sizable fraction of isolated reactants without a partner. Thus, on the basis of statistics, the theoretical maximum yield for solid-state reactions in alternate stacks amounts to 86.5%.[28] The observation of a quantitative yield suggests that this solid-state reaction does not occur randomly with a homogeneous distribution all over the crystal lattice, but rather, it takes place with controlled propagation, that is, progressing either along donor−acceptor stacks in the *x*-axis or along hydrogen bonding in the *y* direction. However, direct experimental proof for such an anisotropic propagation of the reaction is not available at this juncture.[29]

Concluding Remarks

Heteromolecular solid-state reactions can be achieved by the deliberate (i.e., rational) use of electron donor−acceptor or EDA interactions to form mixed charge-transfer crystals prearranged to undergo intermolecular Diels−Alder cycloadditions. Crystal engineering by the judicious choice/design of the donor (anthracene) and acceptor (dithiin) permits the solid-state transformation to be achieved within the same crystal lattice and allows the progressive crystalline change to be precisely monitored by X-ray diffraction methods to high conversions. The monotonic change in activation barrier for solid-state cycloaddition illustrates the direct relationship between crystal arrangements and reactivity, the chain character of solid-state propagation being triggered by the breaking of the C−H···O hydrogen bonds. Such a single-phase transformation allows permanent and predictable lattice control that is sufficient to assemble the cycloaddition product in "anti-thermodynamic" or metastable crystalline form. The latter represents a new kind of topochemical matrix (template) synthesis (predetermined by the reagent packing) and opens the interesting possibility of assembling materials "nonadiabatically" to form artificial crystals with modified properties. Finally, from a somewhat different mechanistic perspective, the progressive crystalline bleaching with conversion proves that the charge-transfer complex itself is the direct precursor to the Diels−Alder adduct, and not an innocent (kinetics) bystander.[30]

Experimental Section

Materials and Methods. Bis(*N*-ethylimino)-1,4-dithiin was prepared and purified by the method of Osawa et al.[20b] The various anthracenes in Figure 1 were obtained from Aldrich and used as received. Benzene and dichloromethane (reagent grade) were stirred over concentrated H_2SO_4 and successively washed with water and aqueous bicarbonate. Benzene was distilled serially from P_2O_5 and from sodium under an argon atmosphere. Dichloromethane was distilled from P_2O_5 and CaH_2. Chloroform (reagent grade) was stirred over several small portions of concentrated H_2SO_4, washed with water, and distilled from P_2O_5 under an argon atmosphere. ^{1}H NMR spectra were recorded in $CDCl_3$ on a General Electric QE-300 NMR spectrometer, and the chemical shifts were reported as ppm downfield from internal tetramethylsilane. UV−vis absorption spectra were recorded on a Hewlett-Packard 8453 diode-array spectrometer.

Formation of Charge-Transfer Complexes. The Mulliken plot[23] in Figure 1 was obtained as follows: To 10 mL solution of **1** (10 mM) in dichloromethane, 10 mL of 0.1 M solutions of various anthracenes (9-Br, H, Me, and 9,10-diMe-anthracene) were added. In each case, λ_{max} for the CT absorption band was determined by subtracting the absorption spectra of pure anthracene and pure 1,4-dithiin solution from that of the mixture. The transition energies ($E_{CT} = hc/\lambda_{max}$) were plotted versus the ionization potentials (IP) of the anthracenes according to the Mulliken correlation.[23] For the preparation of the Job plot in Figure 2, the concentration of the two solutions of 1,4-dithiin and anthracene that were used for the reactions was 20 mM in dichloromethane. The absorbance at $\lambda_{max,CT} = 485$ nm was measured for various molar fractions of anthracene and 1,4-dithiin, and the absorbance values were plotted versus the molar fraction [%] of anthracene.

Preparation of Heteromolecular Single Crystals of Anthracene and Dithiin. The charge-transfer crystal of 1,4-dithiin and anthracene was grown in dichloromethane solution (50 mM) by slow evaporation of the solvent at low temperature (−4 °C). After one week, a brown single crystal was isolated and found to be suitable for multiple X-ray analyses during the course of the solid-state reaction.

Diffuse-Reflectance Spectroscopy of Charge-Transfer Crystals. Freshly prepared 1:1 cocrystals of anthracene and the dithiin were ground into a fine powder and then diluted (5 wt %) with a fine colorless powder of KPF_6. The diffuse-reflectance UV−vis spectrum was recorded on a Varian Cary 5G spectrometer equipped with an integrating sphere.

X-ray Crystal Analysis. The intensity data were collected at −150 °C with a Siemens SMART diffractometer equipped with a 1 K CCD detector using Mo Kα radiation ($\lambda = 0.71073$ Å). The experiments were done on (a) a freshly crystallized sample of the complex; (b) a single crystal of the complex treated for 2h at 50 °C, (c) the same crystal of the complex treated for another 2h at 50 °C, (d) the same crystal of the complex treated for 2 more hours at 50 °C (6 h of thermal treatment, total), and (e) a freshly crystallized sample of the product. The structures of (a) and (e) were solved by direct methods[31] and conveniently refined by a full-matrix least-squares procedure with IBM Pentium and SGI O_2 computers.

Atomic coordinates of the reactants for experiments b−d were taken from the native (unreacted) structure (a), and the structure of the product was found in a series of difference Fourier syntheses as a contaminant superposition of two centrosymmetrically superimposed components.[32] Positions of some atoms superimposed at distances beyond experimental resolution were added geometrically. The superimposed structures (b−d) were refined with reasonable geometrical restrictions using appropri-

(28) (a) Harris, K. D. M.; Thomas, J. M. *J. Chem. Soc., Faraday Trans.* **1991**, *87* (2), 325. (b) Savion, Z.; Wernick, D. L. *J. Org. Chem.*, **1993**, *58*, 2424.

(29) Such a reaction pattern may be directly observed by electron microscopy.

(30) Compare: Fukuzumi, S.; Kochi, J. K. *Tetrahedron*, **1982**, *38*, 1035.

(31) Sheldrick, G. M. *SHELXS-86, Program for Structure Solution*; University of Göttingen: Germany, 1986.

ate options of the SHELXL program package:[33] (i) Total population of the superimposed structures of the complex and the product were kept equal to unity; populations of the two disordered components of the product were kept equal to each other. (ii) Planarity constraints were applied for benzenoid and five-membered imino rings of the product molecule; their geometry was constrained to be the same as that of the parent moieties of the reactants. (iii) Thermal atomic coefficients of closely superimposed atoms of the molecule of the product were restrained to be the same as in the parent reactant molecules. (iv) A riding and rotating model was applied to position all hydrogen atoms with $U_{iso} = 1.2\ U_{iso/eq}$ of an adjacent carbon atom (1.5 $U_{iso/eq}$ for the methyl hydrogens). The pertinent crystallographic data are on deposit at the Cambridge Crystallographic Data Center, U.K.

X-ray Powder Diffraction Study. The samples for the X-ray−powder diffraction were taken as small samples from the same freshly crystallized batch of the complex which was heated incrementally at 50 °C. Between the heating cycles and measurements, the mother batch was stored at room temperature. Powder X-ray diffraction patterns of the samples were recorded at room temperature with a Phillips 1840 powder diffractometer using Cu Kα radiation ($\lambda = 1.54178$ Å) in 0.02° steps over the range $3° < 2\theta < 50°$. The history of the samples is presented in Table 4, together with the degree of conversion determined by ^{1}HNMR spectroscopy. An X-ray diffraction pattern of the recrystallized product was also measured as a standard for comparison.

Kinetics Evaluation of the Solid-State Reactions. Single crystals of the 1,4-dithiin−anthracene complex were ground and placed (in 10-mg portions) into 20 NMR tubes. The NMR tubes were kept in a thermostated water bath at the specified temperature. Periodically, a tube was removed from the bath and the solid contents dissolved in $CDCl_3$ to record the NMR spectrum. The conversion at a given temperature was then calculated from the decrease of the ^{1}HNMR resonances of the 9- and 10-protons of anthracene.

Table 4. Thermal History of Samples Used for X-ray Powder Diffraction Measurements

sample	a	b	c	d	e	f	g	h	i
total time at 50 °C (h)	0	2	4	6	8	10	11	11	15
total time after crystallization (h)	0	25	28	47	51	53	69	121	145
conversion %	0	12.0	17.2	28.6	46.9	70.5	92.6	92.7	100

Kinetics Evaluation of the Solution-Phase Reaction. A 0.5-mL aliquot of a stock solution (50 mM) of 1,4-dithiin and 2 mL of a solution of anthracene were mixed in a 1-cm quartz cell, which was thermostated in a water bath at a given temperature. The concentration of anthracene was in large excess (35−75 times) over that of 1,4-dithiin, and the rates were measured by following the disappearance of the CT band at 485 nm. Pseudo-first-order rate constants (k_{obs}) were extracted from the slopes of the linear plots of $\ln[(A_t - A_\infty)/(A_0 - A_\infty)]$ versus time by a least-squares method, where A_t is the absorbance at time t and A_∞ is the absorbance after 10 half-lives. The first-order rate constant (k_1) and the equilibrium constant (K) were then obtained from a plot of $[k_{obs}]^{-1}$ versus the reciprocal anthracene concentration (see Scheme 2).

Acknowledgment. We thank the National Science Foundation and the Robert A. Welch Foundation for financial support. We are grateful to a referee for pointing out the ambiguity in the product (phase) composition, which necessitated the additional powder-diffraction measurements. We thank Prof. L. Kevan for the use of his X-ray powder diffractometer.

JA001939N

(32) Apparently, the structure of the product resulting from the topochemical reaction belongs to a noncentrosymmetric space group *P*1 (see Figure 7a). However, in our study it appears as a centrosymmetric twin, or centrosymmetrically disordered structure, with equal populations of the components. This type of twinning−disorder may be expected from statistical considerations because the parent structure of the complex is centrosymmetric.

(33) Sheldrick, G. M. *SHELXL-93, Program for Refinement of Crystal Structures*; University of Göttingen: Germany, 1993.